Noise Amplitude Distribution of Impulsive Noise from Measurements in a Power Substation

Qingshan Shan, Shahzad Bhatti, Ian A Glover, Robert Atkinson, Philip J Moore
Dept. of Electronic & Electrical Engineering, University of Strathclyde, 204 George Street, Glasgow, G1 1XW, UK
E-mail: qingshan.shan@eee.strath.ac.uk

Iliana E Portugues
Elimpus Ltd , 28 Wren Court, Strathclyde Business Park, Bellshill, Lanarkshire ML4 3NQ, UK
E-mail: i.portugues@elimpus.com

Richard Rutherford
Scottish Power, Energy, Networks & Telecommunications,1 Atlantic Quay, Glasgow G2 8SP, UK
E-mail: Richard.Rutherford@sppowersystems.com

***Abstract*-This paper presents ultra-wide-band measurements of impulsive noise within an electricity substation compound. The measurements are made in four contiguous frequency bands covering the range 100 MHz to 6 GHz. This range includes those bands relevant to modern wireless LAN and wireless PAN technologies such as IEEE 802.11a/b/g and IEEE802.15.1/4. Impulsive events are extracted from the measured data. A noise amplitude distribution analysis of these events is presented.**

***Index Terms*--Electricity substation, impulsive noise, noise amplitude distribution, ultra-wide-band measurement, wavelet packet, WLAN, WPAN.**

I. Introduction

Impulsive noise has the potential to degrade the performance and reliability of wireless communications systems [1]. Such noise, which is especially prevalent in high-voltage electricity substations, has discouraged the deployment of wireless technologies for operational purposes in the electricity supply industry (ESI). A model of impulsive noise specific to electricity substations would allow the assessment of risk associated with such deployment for monitoring and control functions. Much effort has already been devoted to the measurement of impulsive noise in a variety of physical environments, spanning various frequency bands, with a view to assessing its impact on a range of wireless communication technologies. The environments include urban [1], rural [2], industrial [1], medical [3] and commercial [4]. The bands lie in the between 40 MHz and 4 GHz and the wireless communication technologies include satellite-mobile [2], digital TV [5] and UMTS [6]. In all these campaigns the measurement bandwidths have been relatively narrow, ranging from 120 kHz to 40 MHz.

In this paper we present ultra-wideband measurements of impulsive noise in the specific environment of a 400/275/132 kV air-insulated substation. The data collected will allow the impact on performance of virtually all wireless technologies operating in frequency bands up to 6 GHz to be assessed. These include WiFi (and other WLAN systems), Bluetooth, ZigBee and UWB. The operating frequencies of these technologies, as defined by the IEEE standards 802.11a/b/g [7], 802.15.1 [8] and 802.15.4 [9], respectively, are listed in Table 1. The authors are not aware of any existing measurements that can be used to assess the resilience of these modern wireless technologies to the particular impulsive noise environment found in electricity substations.

Within substations, impulsive noise may occur due to partial discharge (PD), periodic processes from power electronics and lower frequency, sporadic events due to switching operations. The emphasis in this study, however, is on the aggregate impulsive noise background irrespective of its physical origin. Whilst impulsive noise power is strong close to its source it decays rapidly with distance [10]. To characterise it properly, therefore, may require its extraction from a mixture of other unwanted signals and noise processes including coherent interference (e.g. broadcasting, other radio communications and radar signals). This makes practical site-characterisation difficult since impulsive noise sources may be far from buildings where measurement equipment can be protected against environmental effects (in particular humidity and the ingress of water). An effective method of extracting impulsive noise from a background of higher-power noise and interference is therefore desirable. Several methods of extracting PD from other noise processes have been investigated [11] and the wavelet transform has been identified as being particularly useful [12]. The wavelet packet transform (WPT) represents a generalisation of the wavelet transform [13]. An application of WPT for online PD detection in 11 kV cables has been reported [14]. WPT has been used in conjunction with neural networks to separate corona from PD in a gas-insulated substation [15].

TABLE I
Operation Frequency Range Defined by IEEE Standards

802.11a (GHz)	802.11b/g (GHz)	802.15.1 (GHz)	802.15.4 (GHz)
5.15 - 5.25	2.4 – 2.4835	2.4 – 2.4835	0.868 – 0.8686
5.25 - 5.35			2.4 – 2.4835
5.47 - 5.725	2.471 – 2.497 (Japan)		0.902 – 0.928 (USA)
5.725 - 5.825			

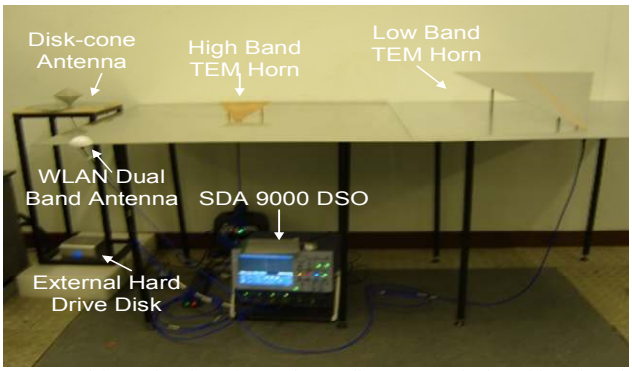

(a) Impulsive noise detection and recording system deployed in substation control room

(b) Strathaven substation – 400 kV compound

Fig. 1. Measurement system and site.

II. Measurement Campaign

An impulsive noise detection system has been developed. The system comprises a low-band (LB) TEM half-horn antenna, a high-band (HB) TEM half-horn antenna, a disk-cone antenna, a WLAN dual-band (2.4/5 GHz) antenna, a high-bandwidth (6 GHz) digital storage oscilloscope (DSO) and a 1 TB external hard disk drive (HDD). The system is shown deployed in a 400 kV substation control room in Fig. 1(a).

The TEM half-horn was selected as the principal antenna type for the collection of data because of its excellent impulse response. Details of the TEM half-horn design were reported in [16]. A summary is repeated here, however, and a schematic diagram is shown in Fig. 2(a).

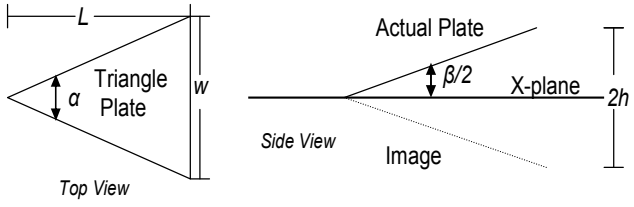

(a) TEM horn

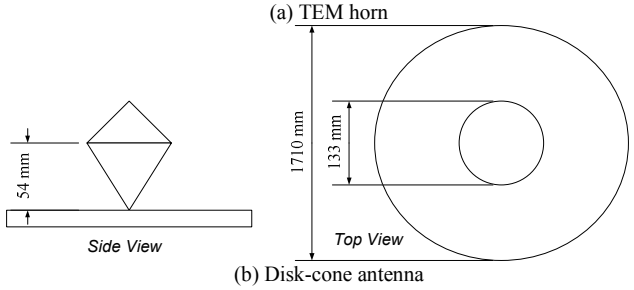

(b) Disk-cone antenna

Fig. 2. Schematic diagrams of antennas.

The LB horn is constructed from a triangular aluminum plate and a 122cm×122cm aluminum ground plane. The width (w) of the triangular plate at the aperture is 65.1cm, its length (L) is 84cm and its aperture height measured from the ground plane (h) is 20.1cm. The antenna feed is a 50Ω SMA connector with its flange in electrical contact with the ground plane and its centre-conductor connected to the triangular plate apex. The amplitude response, measured using a network analyzer, shows the -3dB bandwidth of a pair of identical cascaded horns (transmit and receive) to be 1.264 GHz covering the frequency range 716 MHz - 1.98 GHz. The peak value of the amplitude response occurs at 1.068 GHz.

The HB horn triangular flange is constructed from a printed circuit board. The flange width (w) at the aperture is 21.7cm and its length (L) is 28cm. The aperture height (h) is 6.7cm. The feed structure and ground plane are identical to those of the LB horn. The -3dB bandwidth of a cascaded pair (transmit and receive) is 3.195 GHz (1.905 to 5.1 GHz) and the amplitude response peak value occurs at 2.13 GHz.

The disk-cone antenna covers frequencies below 710 MHz. This is the frequency range conventionally assumed to be important for PD. The details of this antenna design were reported in [17] but are, again, summarized here. A schematic diagram of the disk-cone antenna is shown in Fig. 2(b).

The disk-cone antenna consists of an inverted right circular cone over a circular ground plane. The ground plane is 171cm in diameter and is constructed from aluminium plate. The cone was machined from solid aluminium. It has a base diameter of 13.3cm and heights of 5.4 and 4.9 cm for lower and upper sections of the cone respectively. A non-inverted cone with equal base diameter sits on top of the inverted cone. The antenna is vertically polarised and has approximately flat frequency response in the range 10 MHz - 1 GHz with approximately constant (50 Ω) impedance [18].

A commercial dual-band (DB) omnidirectional antenna designed for WLAN applications is also deployed. It has two passbands sufficiently wide to accommodate WLAN signals in the 2.4 and 5 GHz bands.

The DSO is a LeCroy SDA 9000 with four simultaneous sampling channels. Each channel has a sampling rate of 20 GS/s and 50 MSamples of RAM. The analogue bandwidth is 6 GHz and the input impedance is 50 Ω.

The antennas are connected (directly) to the DSO. Direct sampling is used since previous studies, e.g. [19], have shown this to be advantageous in terms of minimising signal distortion. Interconnection is with 18 GHz, 50 Ω, coaxial cables. Time series are recorded using conventional amplitude triggering. Each recorded time series is 2.5 ms in duration which is the longest possible using the available RAM. The recorded signals are saved to the external HDD which is connected to the DSO via a USB interface.

The measurement site is Strathaven 400/275/132 kV air-insulated substation in the UK, owned by Scottish Power Ltd.

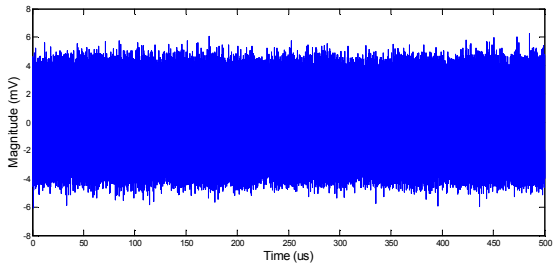

(a) Raw measurement

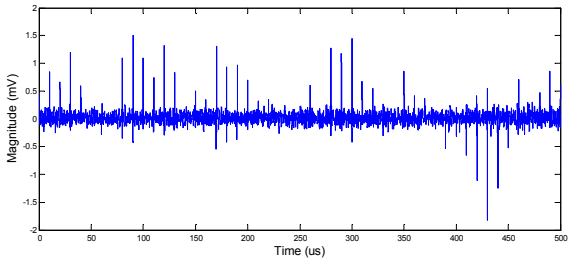

(b) De-noised impulses

Fig. 3. Raw measurement and de-noised result.

Fig. 1(b) is shows a composite image of the 400 kV compound. The site also contains a 275 kV compound (out of shot behind the camera) and a 132 kV compound (out of shot to the left). The 400 kV control building, in which the measurement system was deployed, is shown on the left in Fig. 1(b).

An example of raw data measured in the electricity substation is shown in Fig. 3(a). The abscissa represents sampling time (in μs) while ordinate represents signal level (in mV).

III. Extraction of Impulsive Noise Events

Two stages of data processing are employed to extract impulsive events. The first separates impulsive from non-impulsive 'noise' processes. We refer to this as 'de-noising'. The second extracts the important pulse parameters including rate, amplitude, duration, rise-time, arrival time and spacing. Arrival time is measured with respect to the start of the 2.5 ms data segment.

Due to computer resource constraints (CPU 2.33GHz, 1GB RAM) each time-series record of 5×10^7 samples is divided into five segments containing 10 M samples prior to processing. Fig.3 (a) shows an example time-series record.

A. De-noising

Wavelet packet transformation is central to the extraction of impulses from the measurement records [20]. The signal processing involves four steps. These are:

1) *Decomposition of both approximation and detail*: Wavelet packet decomposition of the signal is computed up to level 12 using the symlet-6 wavelet (as shown in Fig. 4).

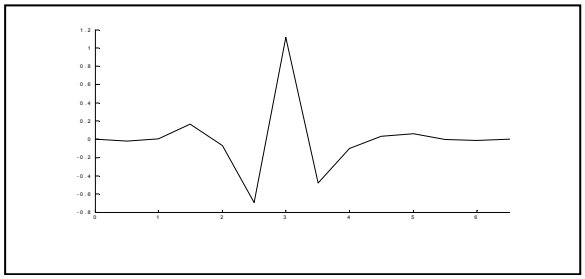

Fig. 4. Symlet-6 wavelet.

2) *Computation of best tree*. The optimal wavelet packet tree with Stein's unbiased risk estimate (SURE) entropy function is computed.
3) *Wavelet-packet coefficient thresholding*: Hard thresholding is applied to the coefficients of each packet (except for the approximation).
4) *Reconstruction*: The required signal is reconstructed based on the original approximation coefficients at each level and the modified detail coefficients

An example of de-noised impulses, extracted from the measurement shown in Fig. 3(a), is given in Fig. 3(b).

B. Extraction of impulse feature

The volume of data measured is large (12 TB) and the volume processed to date is 500 GB. The feature extraction algorithm is therefore required to be computationally efficient in order to keep processing costs manageable. The basic feature extraction algorithm developed in this study comprises the following seven steps:

1) *Calculation of threshold value:* Threshold value, T, is the lesser of T_1 and T_2. T_1 and T_2 are given by

$$T_1 = \frac{1}{k}\max\left|X_j - \frac{\sum_{i=1}^{N} X_i}{N}\right| \tag{1}$$

and

$$T_2 = \frac{l}{N}\sum_{j=1}^{N}\left|X_j - \frac{\sum_{i=1}^{N} X_i}{N}\right| \tag{2}$$

where X is the de-noised time-series, N is the number of samples, $j = 1, 2\ldots N$, and $k = 4$ and $l = 6$.

2) *Identification of time index clusters*: Transition data, M_j, is defined by

$$M_j = X_j - \frac{\sum_{i=1}^{N} X_i}{N} \tag{3}$$

A cluster is identified as a set of contiguous data points satisfying $|M_j| > T$. The values of X_j

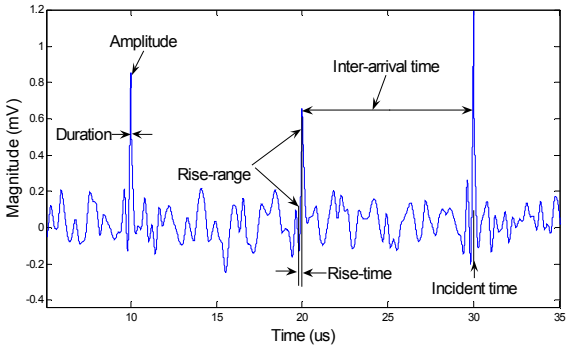

Fig. 5. Illustration of impulse features.

corresponding to one time index cluster are assumed to represent one impulse.

3) *Extraction of impulse amplitude*: Impulse amplitude is the maximum value of X_j within a given time index cluster.
4) *Extraction of impulse occurrence time*: The occurrence time of an impulse is the time index (measured from the start of the data-segment) corresponding to the maximum value of the time cluster.
5) *Calculation of impulse duration*: Impulse duration is the difference of time indices corresponding to locations on either side of the maximum value that are $1/\sqrt{2}$ of the maximum value.
6) *Calculation of impulse rise-time*: Rise-time is the difference of time indices corresponding to 10% and 90% of the pulse's maximum amplitude.
7) *Calculation of inter-arrival time between impulses*: The inter-arrival time is the difference of occurrence times between two successive impulses.

The impulse features are illustrated in Fig. 5, which is a time-dilated segment of Fig. 3(b).

IV. Noise Amplitude Distribution

There are four popular ways of characterizing impulsive noise: envelope peak voltage (PV), quasi-peak voltage (QPV), noise amplitude exceedance (NAE) and noise amplitude distribution (NAD) measurements. A NAD representation of impulsive noise has distinct advantages over the others and contains information about the rate of occurrence of the noise impulses as well as their strength [2].

The ordinate of a NAD curve shows the noise impulse spectral amplitude (usually in decibels above 1 μV/MHz) and the abscissa indicates (usually on a logarithmic scale) the average number of impulses per second that exceed each of the spectral amplitude levels. The (one-sided) voltage spectral amplitude of an impulse envelope in V/Hz is given by $Q = 2A$ where A is the strength (i.e. area) of the envelope measured in Vs. For example, an impulse of 60 dB μV/MHz is equivalent to 10^3 μV/MHz or 10^{-9} V/Hz. This corresponds to a pulse strength of 5×10^{-10} Vs. When a pulse with large bandwidth is present at the input of a receiver with much smaller bandwidth then the peak amplitude of the pulse at the receiver output, v_{pk}, is proportional to the receiver bandwidth, B, i.e., $v_{pk} = QB$. Thus an impulse of spectral amplitude 60 dB μV/MHz will produce a peak voltage at the output of a 1 MHz bandwidth receiver of $10^{-9} \times 10^6 = 10^{-3}$ V. This impulse response will have a duration of approximately twice the reciprocal of the receiver bandwidth, i.e., about 2 μs [21]. Fig. 6 shows an impulse in the time domain. The impulse strength is represented by the shaded area.

A NAD analysis has been undertaken based on data extracted from 318 instances of measured data. The resulting NAD curves are shown in Fig. 7. The average impulse rates corresponding to exceedance values of 75, 60 and 40 dBμV/MHz for each antenna are given in Table 2.

The NAD curves are remarkably similar for all antennas. The mean rate of impulses exceeding 80 dBμV/MHz is

TABLE II
Average Impulse Rate (s^{-1}) Exceeded

NAD (dBμV/MHz) / Antenna	75	60	40
Diskcone	1.26	304	39824
Low-band TEM horn	3.77	273	74707
High-band TEM horm	5.03	118	34794
Dual-band omnidirectional	2.52	25	19990

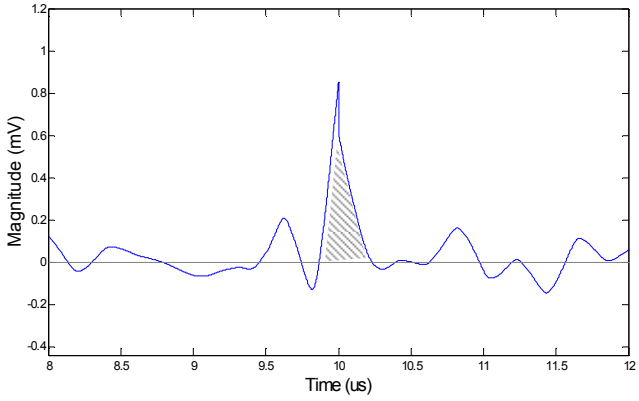

Fig. 6. Illustration of impulse strength.

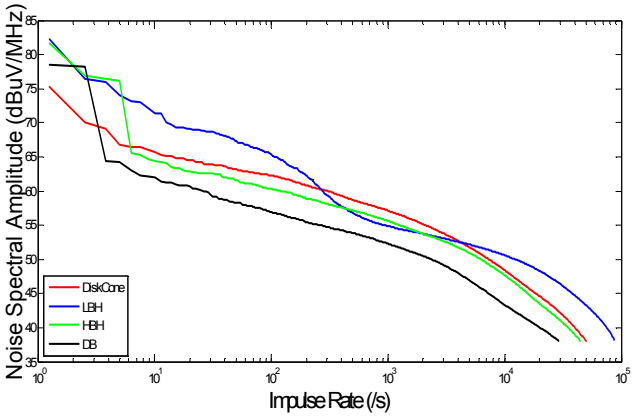

Fig. 7. NAD curves.

approximately 1 Hz. The curve falls at rate of 8 dB/decade to 40 dBμV/MHz at 100 kHz.

V. Conclusion

Impulsive noise has been measured in a 400/275/132 kV electricity substation. The impulsive events have been extracted from raw measurements using a de-noising process and a feature extraction algorithm. NAD curves have been obtained and presented.

An impulsive noise model for the assessment of risk associated with the deployment of wireless communications equipment in substations is under construction.

Acknowledgment

The UK Engineering & Physical Sciences Research Council (EPSRC) is gratefully acknowledged for financial support of this project under Grant EP/D049687/1.

References

[1] M. G. Sanchez, I. Cuinas, and A. V. Alejos, "Interference and impairments in radio communication systems due to industrial shot noise," in *Industrial Electronics, 2007. ISIE 2007. IEEE International Symposium on*, 2007, pp. 1849-1854.

[2] M. D. Button, J. G. Gardiner, and I. A. Glover, "Measurement of the impulsive noise environment for satellite-mobile radio systems at 1.5 GHz," *Vehicular Technology, IEEE Transactions on,* vol. 51, pp. 551-560, 2002.

[3] T. K. Blankenship and T. S. Rappaport, "Characteristics of impulsive noise in the 450-MHz band in hospitals and clinics," *Antennas and Propagation, IEEE Transactions on,* vol. 46, pp. 194-203, 1998.

[4] K. L. Blackard, T. S. Rappaport, and C. W. Bostian, "Measurements and models of radio frequency impulsive noise for indoor wireless communications," *Selected Areas in Communications, IEEE Journal on,* vol. 11, pp. 991-1001, 1993.

[5] M. G. Sanchez, L. de Haro, M. C. Ramon, A. Mansilla, C. M. Ortega, and D. Oliver, "Impulsive noise measurements and characterization in a UHF digital TV channel," *Electromagnetic Compatibility, IEEE Transactions on,* vol. 41, pp. 124-136, 1999.

[6] M. G. Sanchez, A. V. Alejos, and I. Cuinas, "Urban wide-band measurement of the UMTS electromagnetic environment," *Vehicular Technology, IEEE Transactions on,* vol. 53, pp. 1014-1022, 2004.

[7] "IEEE Standard for Information technology-Telecommunications and information exchange between systems-Local and metropolitan area networks-Specific requirements - Part 11: Wireless LAN Medium Access Control (MAC) and Physical Layer (PHY) Specifications," *IEEE Std 802.11-2007 (Revision of IEEE Std 802.11-1999),* pp. C1-1184, 2007.

[8] Bluetooth SIG, "Specification of the Bluetooth System," pp. 1 - 1420, 26 July 2007.

[9] "IEEE Standard for Information technology- Telecommunications and information exchange between systems- Local and metropolitan area networks- Specific requirements Part 15.4: Wireless Medium Access Control (MAC) and Physical Layer (PHY) Specifications for Low-Rate Wireless Personal Area Networks (WPANs)," *IEEE Std 802.15.4-2006 (Revision of IEEE Std 802.15.4-2003),* pp. 0_1-305, 2006.

[10] M. Hikita, H. Yamashita, T. Hoshino, T. Kato, N. Hayakawa, T. Ueda, and H. Okubo, "Electromagnetic noise spectrum caused by partial discharge in air at high voltage substations," *Power Delivery, IEEE Transactions on,* vol. 13, pp. 434-439, 1998.

[11] S. Sriram, S. Nitin, K. M. M. Prabhu, and M. J. Bastiaans, "Signal denoising techniques for partial discharge measurements," *Dielectrics and Electrical Insulation, IEEE Transactions on [see also Electrical Insulation, IEEE Transactions on],* vol. 12, pp. 1182-1191, 2005.

[12] L. Satish and B. Nazneen, "Wavelet-based denoising of partial discharge signals buried in excessive noise and interference," *Dielectrics and Electrical Insulation, IEEE Transactions on [see also Electrical Insulation, IEEE Transactions on],* vol. 10, pp. 354-367, 2003.

[13] S. Mallat, *A wavelet tour of signal processing*, 2nd ed. London: Academic Press, 1999.

[14] A. Kyprianou, P. L. Lewin, V. Efthimiou, A. Stavrou, and G. E. Georghiou, "Wavelet packet denoising for online partial discharge detection in cables and its application to experimental field results," *Measurement Science and Technology,* vol. 17, pp. 2367-2379, 2006.

[15] C. S. Chang, J. Jin, C. Chang, T. Hoshino, M. Hanai, and N. Kobayashi, "Separation of corona using wavelet packet transform and neural network for detection of partial discharge in gas-insulated substations," *Power Delivery, IEEE Transactions on,* vol. 20, pp. 1363-1369, 2005.

[16] Q. Shan, I. A. Glover, P. J. Moore, I. E. Portugues, M. Judd, R. Rutherford, and R. J. Watson, "TEM Horn Antenna for Detection of Impulsive Noise," in *EMC Europe 2008*, Hamburg, Germany, 2008.

[17] P. J. Moore, I. Portugues, and I. A. Glover, "A nonintrusive partial discharge measurement system based on RF technology " in *Power Engineering Society General Meeting, 2003, IEEE*, 2003, p. 633 Vol. 2.

[18] I. Portugues, P. J. Moore, I. A. Glover, C Johnstone, R H McKosky, M B Goff and L V Zel, "Rf-based partial discharge early warning system for air-insulated substations " *IEEE Transactions on Power Delivery, Vol. 24 No. 1, 2009,* pp.20-29.

[19] I. E. Portugues, P. J. Moore, and I. A. Glover, "An investigation into the effect of receiver bandwidth for the interpretation of partial discharge impulses using remote radio sensing," in *International University Power Engineering Conference*, 2002, pp. 529-533.

[20] Q. Shan, S. Bhatti, I. A. Glover, R. Atkinson, I. E. Portugues, P. J. Moore, and R. Rutherford, "Extraction of Impulsive Noise from Measurements in a 400 kV Electricity Substation," *Proceedings of the 4th IASME/WSEAS International Conference on Energy and Environment,* Cambridge, UK, 2009, pp. 135-139.

[21] S. Oranc, "Ignition noise measurements in the VHF/UHF bands," *IEEE Trans. Electromagn. Compat., vol EMC-17,* pp. 135-139, May 1975.